WHEEL/RAIL INTERACTION DUE TO THE POLYGONAL WHEEL

Traian MAZILU[1], Mădălina DUMITRIU[2], Cristina TUDORACHE[3], Mircea SEBEŞAN[4]

Articolul de față este consacrat studierii interacțiunii dintre o osie elastică şi o cale balastată cauzată de roțile poligonale. Osia este considerată o grindă Timoshenko având corpuri rigide fixate de ea reprezentând cutiile de osie, roțile şi discurile de frână. Modelul căii include un nou model al reazemului periodic al şinei constând din două sisteme Kelvin-Voigt tri-direcționale pentru suportul de şină şi balast, şi un sistem mixt Kelvin-Voigt/Maxwell pentru terasament. Principalele caracteristici ale vibrației roată-şină datorită roții poligonale sunt analizate utilizând o nouă tratare a metodei matricei Green a căii.

The paper aims at studying the interaction between an elastic wheelset and ballasted track due to the polygonal wheels. The wheelset is considered a Timoshenko beam with attached rigid-bodies as axle boxes, wheels and brake discs. The track model includes a new model of the rail periodic support consisting in two three-directional Kelvin-Voigt systems for the rail pad and the ballast, and a mixed Kelvin-Voigt/Maxwell system for the subgrade. The main features of the wheel/rail vibration due to the polygonal wheel are analyzed via a new approach of the Green's matrix of the track method.

Key words: ballasted track, wheelset, polygonal wheel, Green's matrix

1. Introduction

Upon studying the dynamic behaviour between the railway vehicle and the track, we may find the responses to many issues such as the passengers' comfort, the rolling noise, the structures' mechanical resistance (the vehicle and the track) and the propagation of the vibrations induced by the trains to the buildings located in the track environment [1-3].

One of the common defects in the railway wheel is the so-called out-of-roundness [4] that may take the shape of the corrugation wheel due to tread braking [5], the wheel flat [6-8] or even the polygonal wheel [9-11]. The former wheel defect consists in the periodic diameter variation around the mean value, so

[1] Assoc. Prof., Depart. of Railway Vehicle, University POLITEHNICA of Bucharest, Romania, e-mail: trmazilu@yahoo.com
[2] Assist. Prof., Depart. of Railway Vehicle, University POLITEHNICA of Bucharest, Romania
[3] Assist. Prof., Depart. of Railway Vehicle, University POLITEHNICA of Bucharest, Romania
[4] Eng., METROREX, Bucharest, Romania.

that the wheel circumference is multiple integer of the wavelength of this defect. The spectrum of the polygonal wheel is dominated by a few waves that correspond to 1-5 wavelengths around the wheel circumference, and the amplitudes are in the order of 1 mm. The frequency range of the vibration induced by the polygonal wheels is situated between 5 and 125 Hz when train velocities are in the interval of 50-250 km/h [12].

All railway wheel types are dominated by the common wheel eccentricity (one harmonic). As a general rule, besides this harmonic, the standard solid steel wheels are dominated by the third harmonic, while the rubber spring wheels prevalently exhibit the second harmonic [13]. Many papers suggest that the polygonal wheel of the third order occurs because of the wheel clamping in a three-jaw chuck [5, 14-15].

This paper herein describes the dynamic behaviour between a wheelset moving along a ballasted track due to the polygonal wheels in order to point out the basic feature of this particular excitation mechanism of the wheel/rail system. To this purpose, the wheelset is modelled as a Timshenko beam with attached rigid-bodies as axle boxes, wheels and brake discs [16]. The rail is considered as an infinite Timoshenko beam resting on a periodic support, including rail pad, semi-sleeper, ballast block and the sub-grade effect. The support model is improved compared to the already known models [17-18] and allows simulating the track response for an extended frequency range [19]. The Green matrix of the track method, previously used to simulate the rigid wheel/rail interaction [20] and the simple vehicle/track interaction [21], is developed here for the elastic wheelset/track interaction.

2. The mechanical model and the governing equations

One considers a wheelset with polygonal wheels uniformly running on a smooth, tangent ballasted track. Considering the two sub-systems, the wheelset and the track as symmetric structures, including the wheels defects and the wheel/rail contact forces, the model of the wheel/rail interaction may be reduced to a wheel running on a discretely supported rail (Fig. 1).

The rail is described using an infinite uniform Timoshenko beam on equidistant supports with a span d between them. The parameters for the rail are as follows: the mass per length unit m, the cross-section area S, the area moment of inertia I, the density ρ, theYoung's modulus E, the shear modulus μ and the shear coefficient κ. The distance from the cross-section neutral fibre to the rail foot is h. The loss factor of the rail is neglected. The motion of the rail is described by the column vector $\mathbf{q} = [w(x, t)\ \theta(x, t)]^{\mathrm{T}}$, where $w(x, t)$ and $\theta(x, t)$ stand for the vertical displacement, respectively the rotation of the cross-section; x is the coordinate along the rail and t stands for time.

In terms of the relative displacements between the rail cross-section and the rail pad, the model of the rail pad has three Kelvin-Voigt systems with the elastic constants k_x, k_r and k_α, and the viscous damping constants c_x, c_r and c_α.

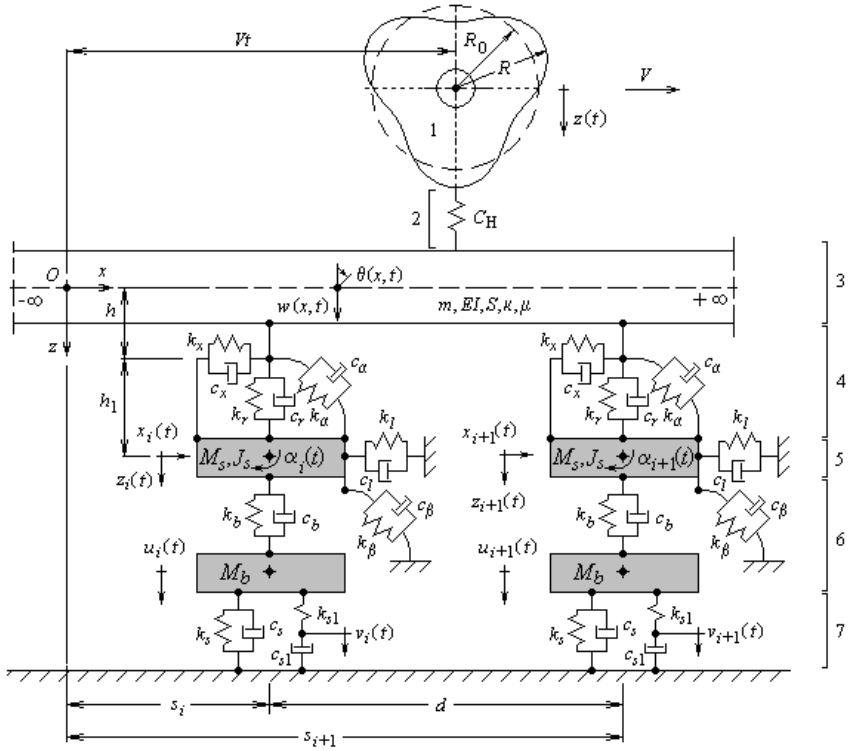

Fig. 1. Mechanical model of the wheel/rail interaction due to the polygonal wheel: (1) polygonal wheel; (2) wheel/rail contact; (3) rail; (4) rail pad; (5) semi-sleeper; (6) ballast; (7) subgrade.

The semi-sleepers are taken as rigid bodies with three degrees of freedom, i.e. the $x_i(t)$ longitudinal translation, the $z_i(t)$ vertical displacement and the $\alpha_i(t)$ rotation across the rail, where i is the sleeper number, situated at the distance s_i from the reference. The parameters for the semi-sleepers are: the mass M_s, the mass moment of inertia J_s and the distance h_1 between the semi-sleeper and the rail pad.

The ballast model consists in a rigid body in the $u_i(t)$ vertical translation under the i semi-sleeper via the Kelvin-Voigt system. The longitudinal and rotational resistance of the ballast are taken into account by using two Kelvin-Voigt systems connected to the semi-sleeper. The ballast model has the mass M_b, the elastic constants k_b, k_l and k_β and the viscous damping constants c_b, c_l and c_β.

Finaly, the subgrade influence is simulated using a mixed Kelvin-Voigt/Maxwell system [19]. This solution is valid as long as the axle velocity is

much lower than the velocity of the waves excited in the subgrade by the axle travel.

The equations of motion for the rail and its periodical supports may be written as

$$\mathbf{T}_{x,t}\mathbf{q}(x,t)-\sum_{i=-\infty}^{\infty}(\mathbf{A}_t\mathbf{q}_i(t)-\mathbf{B}_t\mathbf{q}_i^s(t))\delta(x-s_i)=\mathbf{Q}(x,t) \tag{1}$$

$$\mathbf{C}_t\mathbf{q}_i^s(t)=\mathbf{B}_t^{\mathrm{T}}\mathbf{q}_i(t) \tag{2}$$

where

$$\mathbf{Q}=\left[-Q(t)\delta(x-Vt)\quad 0\right]^{\mathrm{T}} \tag{3}$$

is the column vector of the vertical forces acting on the rail, $\delta(.)$ is the Dirac delta function, $\mathbf{q}_i(t) = \mathbf{q}(s_i,t)$ is the column vector of the rail displacement above the support i, $\mathbf{q}_i^s(t)=\left[x_i(t)\quad z_i(t)\quad \alpha_i(t)\quad u_i(t)\quad v_i(t)\right]^{\mathrm{T}}$ represents the displacements belonging to the support i, including the $v_i(t)$ hidden displacement of the Maxwell system, $\mathbf{T}_{x,t}$ is the matrix differential opperator of the Timoshenko beam

$$\mathbf{T}_{x,t}=\begin{bmatrix}\kappa\mu S\dfrac{\partial^2}{\partial x^2}-m\dfrac{\partial^2}{\partial t^2} & -\kappa\mu S\dfrac{\partial}{\partial x}\\ \kappa\mu S\dfrac{\partial}{\partial x} & EI\dfrac{\partial^2}{\partial x^2}-\kappa\mu S-\rho I\dfrac{\partial^2}{\partial t^2}\end{bmatrix} \tag{4}$$

and $\mathbf{A}_t$, $\mathbf{B}_t$, $\mathbf{C}_t$ stand for the following matrix differential

$$\mathbf{A}_t=\begin{bmatrix}c_r\dfrac{\mathrm{d}}{\mathrm{d}t}+k_r & 0\\ 0 & c_\theta\dfrac{\mathrm{d}}{\mathrm{d}t}+k_\theta\end{bmatrix}; \tag{5}$$

$$\mathbf{B}_t=\begin{bmatrix}0 & c_r\dfrac{\mathrm{d}}{\mathrm{d}t}+k_r & 0 & 0 & 0\\ -h\left(c_x\dfrac{\mathrm{d}}{\mathrm{d}t}+k_x\right) & 0 & \Delta c_\alpha\dfrac{\mathrm{d}}{\mathrm{d}t}+\Delta k_\alpha & 0 & 0\end{bmatrix}; \tag{6}$$

$$\mathbf{C}_t=\begin{bmatrix}D_x & 0 & h_1\left(c_x\dfrac{\mathrm{d}}{\mathrm{d}t}+k_x\right) & 0 & 0\\ 0 & D_z & 0 & -c_b\dfrac{\mathrm{d}}{\mathrm{d}t}-k_b & 0\\ h_1\left(c_x\dfrac{\mathrm{d}}{\mathrm{d}t}+k_x\right) & 0 & D_\alpha & 0 & 0\\ 0 & -c_b\dfrac{\mathrm{d}}{\mathrm{d}t}-k_b & 0 & D_u & -k_{s1}\\ 0 & 0 & 0 & -k_{s1} & D_v\end{bmatrix} \tag{7}$$

with

$$D_x = M_s \frac{\mathrm{d}^2}{\mathrm{d}t^2} + (c_x + c_l)\frac{\mathrm{d}}{\mathrm{d}t} + k_x + k_l;$$

$$D_z = M_s \frac{\mathrm{d}^2}{\mathrm{d}t^2} + (c_r + c_b)\frac{\mathrm{d}}{\mathrm{d}t} + k_r + k_b,\ D_v = c_{s1}\frac{\partial}{\partial t} + k_{s1};$$

$$D_\alpha = J_s \frac{\mathrm{d}^2}{\mathrm{d}t^2} + (c_\alpha + c_\beta + h_1^2 c_x)\frac{\mathrm{d}}{\mathrm{d}t} + k_\alpha + k_\beta + h_1^2 k_x;$$

$$D_u = M_b \frac{\mathrm{d}^2}{\mathrm{d}t^2} + (c_b + c_s)\frac{\mathrm{d}}{\mathrm{d}t} + k_b + k_s + k_{s1};$$

$$c_\theta = c_\alpha + h^2 c_x,\ k_\theta = k_\alpha + h^2 k_x,\ \Delta c_\alpha = c_\alpha - h h_1 c_x,\ \Delta k_\alpha = k_\alpha - h h_1 k_x.$$

All the initial conditions and the boundary conditions are null

$$\mathbf{q}(x,0) = \begin{bmatrix}0 & 0\end{bmatrix}^{\mathrm{T}},\ \mathbf{q}_i^s(0) = \begin{bmatrix}0 & 0 & 0 & 0 & 0\end{bmatrix}^{\mathrm{T}}, \tag{8}$$

$$\lim_{|x-Vt|\to\infty} \mathbf{q}(x,t) = \begin{bmatrix}0 & 0\end{bmatrix}^{\mathrm{T}},\ \lim_{i\to\pm\infty} \mathbf{q}_i^s(t) = \begin{bmatrix}0 & 0 & 0 & 0 & 0\end{bmatrix}^{\mathrm{T}}. \tag{9}$$

The wheelset model is presented in Fig. 2, where a wheelset of a passenger coach with four brake discs is being looked at.

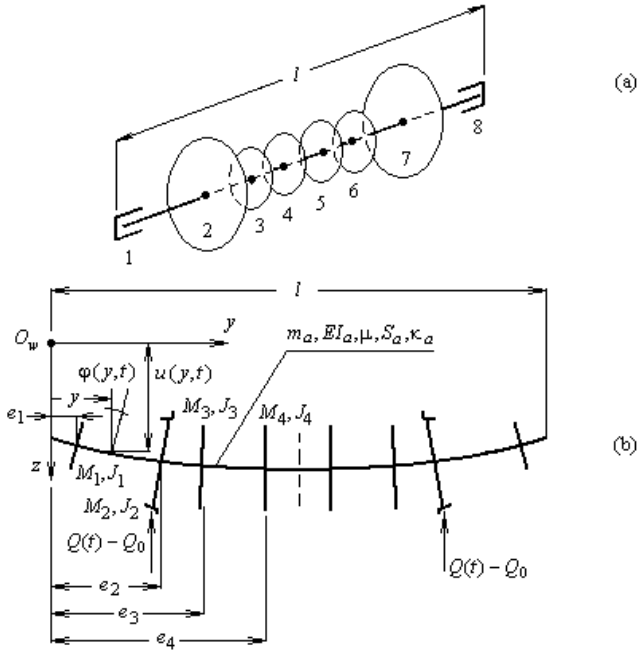

Fig. 2. Mechanical model of the wheelset: (1) and (8) axle box; (2) and (7) wheel; (3-6) brake disc.

The axle is modelled as a uniform Timoshenko beam with attached rigid bodies as wheels, axle boxes and brake discs. The displacements of the axle are described by the column vector $\mathbf{q}^a(y, t) = [u(y, t)\ \varphi(y, t)]^{\mathrm{T}}$, where $u(y, t)$ and $\varphi(y, t)$ are the vertical displacement and the rotation of the cross-section, y stands for the coordinate along the axle. The parameters of the axle are: the Young's modulus E, the shear modulus μ, the density ρ, the length l, the mass per length unit m_a, the cross-section area S_a, the area moment of inertia I_a and the shear coefficient κ_a. The body 'i' ($i = 1 \div 8$) is attached to the axle at the distance e_i from the left end of the axle and has the mass M_i and the mass-moment inertia J_i.

Assuming the wheelset motion around the equilibrium position and neglecting the gyroscopic effects and the static and dynamic imbalances of the wheel set, the governing equations of motion may be written as follows

$$\mathbf{T}^a_{y,t}\mathbf{q}^a - \sum_{i=1}^{8}\mathbf{F}_{i,t}\mathbf{q}^a_i\delta(y-e_i) = \mathbf{Q}^a, \tag{10}$$

where $\mathbf{T}^a_{y,t}$ şi $\mathbf{F}_{i,t}$ are the matrix differential operators, $\mathbf{q}^a{}_i = \mathbf{q}^a(e_i, t)$ is the column vector of the axle displacements at the e_i section and

$$\mathbf{Q}^a = [Q(t) - Q_0][\delta(y-e_2) + \delta(y-e_7)\quad 0]^{\mathrm{T}} \tag{11}$$

is the column vector of the forces acting on the wheels; $Q(t)$ is the wheel/rail contact force, while Q_0 is the static load. The matrix differential operators appearing in the equation of motion of the axle are as follows

$$\mathbf{T}^a_{y,t} = \begin{bmatrix} \kappa_a\mu S_a\dfrac{\partial^2}{\partial y^2} - m_a\dfrac{\partial^2}{\partial t^2} & -\kappa_a\mu S_a\dfrac{\partial}{\partial y} \\ \kappa_a\mu S_a\dfrac{\partial}{\partial y} & EI_a\dfrac{\partial^2}{\partial y^2} - \kappa_a\mu S_a - \rho I_a\dfrac{\partial^2}{\partial t^2} \end{bmatrix} \tag{12}$$

$$\mathbf{F}_{i,t} = \begin{bmatrix} M_i\dfrac{\mathrm{d}^2}{\mathrm{d}t^2} & 0 \\ 0 & J_i\dfrac{\mathrm{d}^2}{\mathrm{d}t^2} \end{bmatrix}. \tag{13}$$

The boundary conditions (free-free) are the same for both ends of the axle ($y = 0$ and $y = l$)

$$\frac{\partial u}{\partial y} - \varphi = 0\,;\ \ \frac{\partial\varphi}{\partial y} = 0\,, \tag{14}$$

which means that the shear force and the moment are null. Also, the initial conditions for the axle are null.

The wheel/rail interaction model has to contain a restriction, due to the hertzian contact between the wheel and the rail. According to Hertz's theory, one reads

$$\left[Q(t)/C_{\mathrm{H}}\right]^{2/3} = z_{\delta}(t)\sigma\left[z_{\delta}(t)\right], \tag{15}$$

where z_δ is the wheel/rail deflection, C_H is the Hertzian constant and $\sigma[.]$ is the unitary step function of *Heaviside*. The wheel/rail deflection may be written as

$$z_{\delta}(t) = z(t) - w(Vt,t) - \Delta r(t), \tag{16}$$

where $z(t) = u(e_2,t)\ ) = u(e_7,t)$ is the wheel displacement and $\Delta r(t)$ stands for the wheel/rail relative displacement due to the polygonal wheel. Neglecting the influence of the deviation (offset) between the contact point and the wheel centre, the wheel/rail relative displacement may be written as

$$\Delta r(t) = \Delta r_0 \cos n(V/R_0)t, \tag{17}$$

where Δr_0 is the amplitude R_0 is the wheel radius and n is an integer corresponding to the order of the polygonal wheel.

3. Solution of equations of motion

The solution of the equations of motion can be obtained by using the Green's matrix of the track method [20-21]. To this end, the Green's function of the wheelset at the wheel has to be calculated following the method suggested by the authors [16]. This function describes the wheel response when two impulse forces are symmetrically applied on the wheels and it has the form below

$$h(t) = \frac{t}{M} + \sum_{i=1}^{N} \frac{1}{M_i} \frac{\exp(-\zeta_i \omega_i t)}{\omega_i \sqrt{1-\zeta_i^2}} \sin\left(\omega_i \sqrt{1-\zeta_i^2}\, t\right), \tag{18}$$

where M is the half-mass of the wheelset, M_i is the modal mass of the i vibration mode, ω_i is the resonance angular frequency and ζ_i is the modal damping factor; the first N modes are taken into account.

Also, one needs the Green's matrix of the track including the response of the rail along a sleeper bay due to a unit moving impulse force. This matrix is assembled by the Green's functions of the rail.

In virtue of the convolution theorem, the wheel displacement and the rail displacement at the moving contact point are given as

$$z(t) = \int_0^t h(t-\tau)\left[Q_0 - Q(t)\right]\mathrm{d}\tau \tag{19}$$

$$w(Vt,t) = \int_0^t \int_{-\infty}^{\infty} g^w(Vt,\xi,t-\tau)Q(\tau)\delta(\xi - V\tau)\mathrm{d}\xi\mathrm{d}\tau = \int_0^t g^w(Vt,V\tau,t-\tau)Q(\tau)\mathrm{d}\tau, \tag{20}$$

where $g^w(Vt,\xi,t\text{-}\tau)$ is the Green's function of the rail at the moving point.

Next, these displacements are introduced in the contact equation (15) and one obtains an integral nonlinear equation with the contact force as unknown

$$\left[Q(t)/C_{\mathrm{H}}\right]^{2/3} = \int_0^t h(t-\tau)\left[Q_0 - Q(t)\right]\mathrm{d}\tau - \int_0^t g^{w}(Vt, V\tau, t-\tau)Q(\tau)\mathrm{d}\tau - \Delta r(t) \quad (21)$$

The equation is valid as long as the wheel and the rail are in contact and it may be solved following a numerical approach.

4. Numerical application

In this section, results are derived from the previous wheel/rail model for a particular wheelset that uniformly moves along a ballasted track, considering the symmetric polygonal wheels of the third order. The model parameters are listed in Table 1 for the wheelset and in Table 2 for the track.

Table 1

Parameters for the wheelset

Parameter	Value
Density of the axle (steel)	$\rho = 7850$ kg/m^3
Young's modulus of the axle	$E = 210$ GPa
Shear modulus of the axle	$\mu = 81$ GPa
Length of the axle	$l = 2.2$ m
Mass per length unit of the axle	$m_a = 157$ kg/m
Cross-section area of the axle	$S_a = 0.02$ m^2
Area moment of inertia of the axle cross-section	$I_a = 3.22 \cdot 10^{-5}$ m^4
Shear coefficient of the axle cross-section	$\kappa_a = 0.9$
Mass of the axle box	$M_1 = M_8 = 80$ kg
Mass of the wheel	$M_2 = M_7 = 334$ kg
Mass of the brake disc	$M_3 = M_4 = M_5 = M_6 = 70$ kg
Mass moment inertia of the axle box	$J_1 = J_8 = 1$ kgm^2
Mass moment inertia of the wheel	$J_2 = J_7 = 23$ kgm^2
Mass moment inertia of the brake disc	$J_3 = J_4 = J_5 = J_6 = 2$ kg m^2
Positions of the axle boxes	$e_1 = 0.08$ m; $e_8 = 2.12$ m
Positions of the wheels	$e_2 = 0.35$ m; $e_7 = 1.85$ m
Position of the first two brake discs	$e_3 = 0.65$ m; $e_4 = 0.95$ m
Static load	$Q_0 = 70$ kN

For the numerical simulation, the track model length is of 50 sleeper bays; this length satisfies the mandatory criterion to keep the periodic feature of the track in the central zone of the model (14 sleeper bays). Only the rail receptance from this zone is used, with the purpose to calculate Green's matrix of the track.

Table 2

Parameters for the track

Parameter	Value
Mass per length unit of the rail	$m = 60$ kg/m
Cross-section area of the rail	$S = 7.69 \cdot 10^{-3}$ m^2
Area moment of inertia of the rail cross-section	$I = 30.55 \cdot 10^{-6}$ m^4
Shear coefficient of the rail cross-section	$\kappa = 0.4$
Distance between the cross-section's neutral fibre and the rail foot	$h = 0.08$ m
Longitudinal rail pad stiffness	$k_x = 50$ MN/m
Vertical rail pad stiffness	$k_r = 280$ MN/m
Rotational rail pad stiffness	$k_\alpha = 597$ kNm/rad
Longitudinal rail pad viscous damping constant	$c_x = 10$ kNs/m
Vertical rail pad viscous damping constant	$c_r = 50$ kNs/m
Rotational rail pad viscous damping constant	$c_\alpha = 107$ Nms/rad
Mass of semi-sleeper	$M_s = 145$ kg
Mass-moment of inertia of semi-sleeper	$J_s = 1.28$ kgm^2
Sleeper bay	$d = 0.6$ m
Distance between the semi-sleeper centroid and the rail pad	$h_1 = 0.116$ m
Longitudinal ballast stiffness	$k_l = 40$ MN/m
Vertical ballast stiffness	$k_b = 120$ MN/m
Rotational ballast stiffness	$k_\beta = 676$ kNm/rad
Longitudinal ballast viscous damping constant	$c_l = 52$ kNs/m
Vertical ballast viscous damping constant	$c_b = 70$ kNs/m
Rotational ballast viscous damping constant	$c_\beta = 394$ kNs/m
Mass of ballast block	$M_b = 2500$ kg
Vertical subgrade stiffness (Kelvin-Voigt system)	$k_s = 60$ MN/m
Vertical subgrade stiffness (Maxwell system)	$k_{s1} = 100$ MN/m
Vertical subgrade viscous damping constant (Kelvin-Voigt system)	$c_s = 150$ kNs/m
Vertical subgrade viscous damping constant (Maxwell system)	$c_{s1} = 600$ kNs/m

One considers that the wheel defect has the wavelength of 960 mm, corresponding to a wheel circumference of 2880 mm (wheel diameter about 920 mm). The defect amplitude is 100 μm and this value is currently obtained from the experimental data [5].

Figure 3 shows the wheel displacement and the rail displacement at the contact point during the running at the speed of 62 m/s. The system vibration has two components, one is given by the parametric excitation due to the sleepers with the wavelength of 600 mm, and the other one is initialised by the wheel defect (wavelength of 960 mm). Consequently, the wheel/rail vibration is modulated with the wavelength of 4800 mm, corresponding to the frequency of 12.92 Hz. Notice the parametric frequency of 103.33 Hz and the frequency of 64.58 Hz due to the polygonal wheel. One may observe that the vibration is dominated by the component in the polygonal wheel.

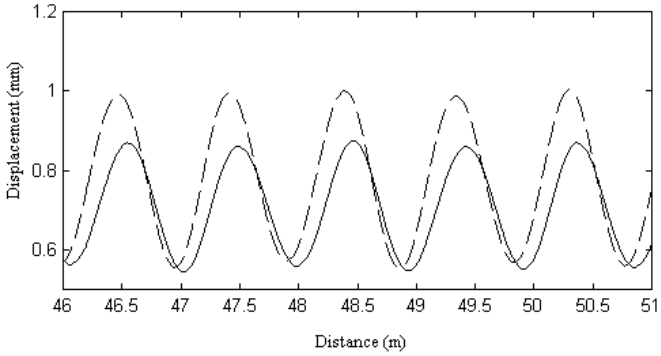

Fig. 3. Wheel/rail displacements at 62 m/s in the presence of the third order polygonal wheel (amplitude of 0.1 mm): —, rail displacement at contact point; – – –, wheel displacement.

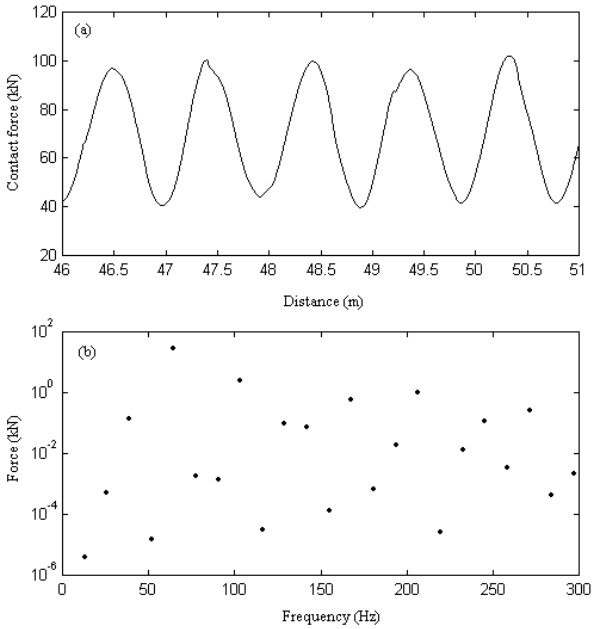

Fig. 4. Wheel/rail contact force at 62 m/s in the presence of the third order polygonal wheel (amplitude of 0.1 mm): (a) the time history; (b) the spectrum.

The time history and the spectrum of the contact force are presented in Fig. 4. The contact force has high oscillations around the static load value; the maximum value is 102 kN and the minimum 39.7 kN. Also, the effective contact force is 20.16 kN, resulting from the numerical simulation. The highest component of the contact force spectrum has the amplitude of 28.4 kN and it comes from the polygonal defect of the wheel (a frequency of 64.58 Hz). The component deriving from the parametric excitation of the sleepers is significant, its amplitude reaching 2.53 kN (frequency of 103.33 Hz). Apart from this, all

components are very low, excepting the second component of the parametric excitation with the amplitude of 0.96 kN (a frequency of 206.7 Hz).

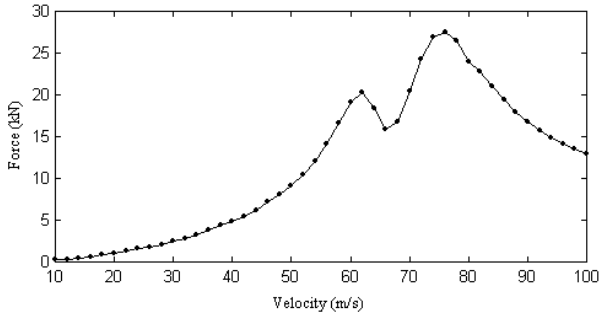

Fig. 5. Wheel/rail effective contact force versus the velocity in the presence of the third order polygonal wheel (the amplitude of 0.1 mm).

Fig. 5 displays the effective contact force versus the wheelset velocity, taking into account the same polygonal wheel. The contact force has two peaks at 62 and 76 m/s corresponding to the resonance frequencies of the wheelset/track system – the resonance due the first symmetric bending mode and the resonance given by the rigid-body mode of the wheelset. In fact, the vibration level turns high for the velocity between 200 km/h and 335 km/h.

When the defect amplitude is higher than a particular value, the contact force leads to the contact loss. Such situation is depicted in Fig. 6 where the results from the numeric simulation of the polygonal wheel/rail interaction are presented for the amplitude of 260 μm and the velocity of 62 m/s. At contact point the wheel and the rail vibrate almost in phase. One remarks the very high level of the contact force showing as periodic shocks. The maximum value is two times higher than the static load.

Finally, the last issue studied here is shown in Fig. 7, where the diagram of the maximum and minimum contact force versus the polygonal wheel amplitude

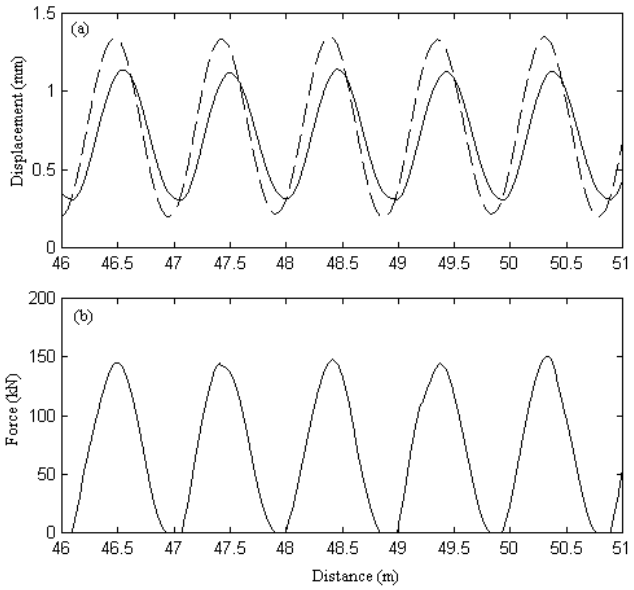

Fig. 6. Wheel/rail interaction due to the polygonal wheel (amplitude of 0.260 mm) at speed of 62 m/s: (a) —, rail displacement at contact point; – – –, wheel displacement; (b) contact force.

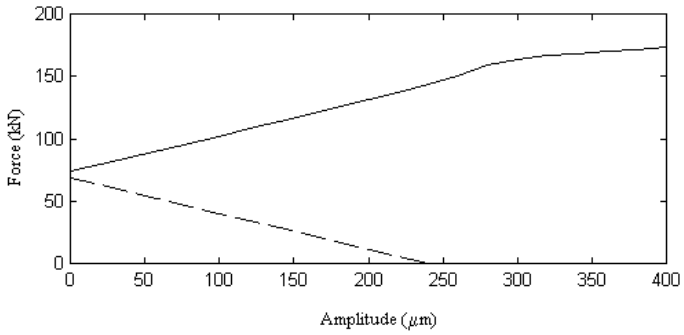

Fig. 7. Maximum and minimum contact force at speed of 62 m/s: —, maximum contact force; – – –, minimum contact force.

is presented. The wheelset velocity of 62 m/s has been taken into account for. Obviously, when the defect amplitude increases, the maximum contact force increases as well, while the minimum contact force decreases. These trends are linear because the elasticity of the contact is much lower than the rail and wheel receptances, and, subsequently, the nonlinear contact has a very marginal influence. When the defect amplitude is higher than 250 μm, the contact loss occurs and the maximum contact force increases linearly but its slope is smaller.

6. Conclusions

The dynamic stresses due to the wheel/rail vibration induced by the irregularities of the rolling surfaces affect the mechanical structure of both vehicle and track.

This paper shows a study meant for the dynamic behaviour of the wheel/rail interaction when the wheels exhibit the third-order polygonal defect. This kind of wheel defect comes from the machine work of the wheels and it is prevalent.

To this end, one considered the case of a wheelset with four brake discs in a passenger coach moving along a ballasted track. The axle is taken as a Timoshenko beam with attached rigid-bodies as axle boxes, wheels and brake discs. Only the symmetric bending modes are taken into account. The time-domain Green's function at the wheel is obtained via the receptance and the modal analysis. The model track is reduced to a discretely supported rail, since the track is considered a symmetric structure. The rail is modelled as an infinite uniform Timoshenko beam. The support of the rail model is improved to extend the results range according to the measurements, both for low and high frequencies. In fact, this model of the periodic support consists in two three-directional Kelvin-Voigt systems for the rail pad and the ballast, and a mixed Kelvin-Voigt/Maxwell system for the subgrade. Also, the inertia of the sleeper and the ballast block is introduced.

The numerical simulations show that the dynamic behaviour due to the polygonal wheel is dominant, while the one from the parametric excitation of the sleepers play a marginal role. The influence of the wheelset velocity consists in two peaks of the effective contact force corresponding to the bending resonance of the wheelset on the track and the resonance of wheelset/track system due to the rigid-body mode of the wheelset. The contact force increases with the amplitude of the wheel irregularity. However, when contact is lost, the contact force lowers.

Acknowledgements

This work was supported by CNCSIS-UEFISCSU, project number 684 PN II – IDEI code 1699/2008: *Researches on the wheel/rail parametric vibrations using the track's Green matrix method.*

R E F E R E N C E S

[1] *I. Sebeşan*, Dinamica vehiculelor feroviare, (Dynamic of the railway vehicles), Ed. Tehnica, Bucureşti, 1995.
[2] *I. Sebeşan, T. Mazilu*, Vibrațiile vehiculelor feroviare, (Vibrations of the railway vehicles), MatrixRom, Bucureşti, 2010.
[3] *T. Mazilu*, Vibrații roată-şină, (Wheel/rail vibrations), MatrixRom, Bucureşti, 2008.

[4] *J. C. O. Nielsen and A. Johansson*, "Out-of-round railway wheels - a literature survey" in Proc. Instn Mech. Engrs, Part F: J. Rail and Rapid Transit, **214**, 2000, pp. 79-91.
[5] *A. Johansson*, "Out of round railway wheels-assessment of wheel tread irregularities in traffic" in Journal of Sound and Vibration **293**, 2006, pp. 795-806.
[6] *R. Dukkipati, R. Dong*, "Impact Loads due to Wheel Flats and Shells" in Vehicle System Dynamics, **31**, 1999, pp. 1-22.
[7] *T. Wu and D. J. Thompson*, "A hybrid model for the noise generation due to railway wheel flats", in Journal of Sound and Vibration, **251** no. 1, 2002, pp. 115-139.
[8] *M. J. M. M. Steenbergen*, "The role of the contact geometry in wheel-rail impact due to wheel flats", in Vehicle System Dynamics, **45**, 2007, pp. 1097-1116.
[9] *A. Johansson, C, Andersson*, "Out of round railway wheels-a study of wheel polygonalization through simulation of three-dimensional wheel-rail interaction and wear", in Vehicle System Dynamics, **43**, 2005, pp. 539-559.
[10] *T. Mazilu*, "Interaction between a moving two-mass oscillator and an infinite homogeneous structure: Green's functions method", in Archive of Applied Mechanics, **80**, 2010, pp. 909-927.
[11] *P. Meinke, S. Meinke*, "Polygonalization of wheel treads caused by static and dynamic imbalances", in Journal of Sound and Vibration **227**, 1999, pp 979-986.
[12] *J.C.O. Nielsen, R. Lunden, A. Johansson, T. Vernersson*, "Train-Track Interaction and Mechanisms of Irregular Wear on Wheel and rail Surfaces", in Vehicle System Dynamics, **40**, 2003, pp. 3-54.
[13] *G. Palgen*, "Unrunde Räder an Eisenbahnfahrzeugen", in Eisenbahningenieur **49**, 1998, pp. 56-60.
[14] *W. Rode, D. Mller and J. Villman*, "Results of DB AG Investigations "Out of Round Wheels", in Proceedings of the Corrugation Symposium-Extended Abstracts, IFV Bahntechnik, Technische Universität Berlin, Germany, 1997.
[15] *W. Mombrei and P Ottlinger*, "Das Unrundwerden von Eisenbahnrädern aus Werkstofftechnischer Sicht-ein Überblick" in ZEV+DET Glasers Annalen **125**, 2001, pp. 59-65.
[16] *T. Mazilu, M. Dumitriu, C. Tudorache and M. Sebeşan*, "Railway wheelset bending flexibility" in Proceedings of the 11 WSEAS International Conference on Automation & Information (ICAI '10), G. Enescu University, Iasi, Romania, June 13-15, 2010.
[17] *W. M. Zhai, K. Y. Wang, J. H. Lin*, "Modelling and experiment of railway ballast vibrations, in Journal of Sound and Vibration **270**, 2004, pp. 673-683.
[18] *J. C. O. Nielsen*, "High-frequency vertical wheel-rail contact forces-Validation of a prediction model by field testing", in Wear, **265**, 2008, pp. 1465-1471.
[19] *T. Mazilu, M. Dumitriu, C. Tudorache and M. Sebeşan*, "On vertical analysis of railway track vibration", in Proceedings of the Romanian Academy Series A, vol. **11** no. 2, 2010, pp. 156-162.
[20] *T. Mazilu*, "Green's functions for analysis of dynamic response of wheel/rail to vertical excitation", in Journal of Sound and Vibration, **306**, 2007, pp. 31–58.
[21] *T. Mazilu*, "Prediction of the interaction between a simple moving vehicle and an infinite periodically supported rail - Green's functions approach", in Vehicle System Dynamics vol. **48**, no. 9, 2010, pp. 1021-1042.